Fiber Bragg gratings for atom chips

Steve Helsby, Costantino Corbari, Morten Ibsen, Peter Horak, and Peter Kazansky
Optoelectronics Research Centre, University of Southampton, Southampton SO17 1BJ, United Kingdom
(Received 21 August 2006; published 17 January 2007)

We discuss the fabrication and characterization of fiber Fabry-Perot cavities developed for integrated atom detection on the atom chip. Investigations show that the cavities are suitable for the detection of small numbers of atoms, with restrictions due to absorption in the Bragg gratings. We show that a significant reduction in these absorption losses can be attained by thermal annealing, removing any material limitations to single-atom detection.

DOI: 10.1103/PhysRevA.75.013618 PACS number(s): 03.75.Be, 32.80.−t, 03.67.−a, 42.81.−i

I. INTRODUCTION

In recent years there has been great progress in the field of trapping and cooling of neutral atoms. This work has led to the "atom chip" [1–4], an integrated device developed to manipulate matter on the quantum scale for the purpose of quantum information processing. Ultracold neutral atoms are held and transported close to the surface of the chip within the magnetic potentials created by the chip's current-carrying wires, with further interaction achieved via permanent magnetic [5] or electrostatically charged elements. For the most part, macroscale optical components have been used to deliver the optical field necessary for coherent atom-state manipulation and atomic investigation [6,7]. Optical fibers present an ideal first step toward the introduction of microoptical replacements for these components due to their low loss and tight optical confinement. Mounted on the chip [8–11] they can provide an optical counterpart to the atom optical elements already present.

The use of an optical cavity to enhance atom-light interactions is a well-known technique, with the Fabry-Perot (FP) resonator being the workhorse of cavity QED experiments. Fiber FP resonators several centimeters long have been suggested for atom detection on atom chips, and it has been shown theoretically that single-atom detection is possible using a fiber resonator with a relatively modest finesse ($F \sim 100$) [12]. This sensitivity is possible due to the strong coupling between the atom and the light afforded by the small radiation-mode waist at the position of the atom ($\sim 2\ \mu$m). The atoms are to be introduced into the cavity via a 5-μm gap, and a change in the intensity or phase of the light output from the cavity due to the presence of an atom will be detected by direct or homodyne measurement, respectively.

Here we are concerned with the fabrication and analysis of such fiber cavities constructed using uniform Bragg gratings which are side-written into single-mode fiber using cw UV light [13,14]. Gratings of various lengths were written using different writing fluences, but each had a design wavelength near to 780 nm, the wavelength of the $D2$ transition in rubidium, a commonly used atom in atom chip experiments. A careful analysis of the characteristics of these gratings was accomplished via measurements made upon the cavities prior to the introduction of the gap. We note here that fine-tuning of the gratings, via stretching or temperature control, will be necessary in a working device in order to operate at the precise wavelength required.

The small ($\sim$2-μm) mode waist and 5-μm gap immediately introduce a minimum loss per pass of $\sim$1% due to diffraction, and any other inherent loss, such as loss in the gratings, will result in a marked reduction in cavity throughput and, more importantly, affect the signal-to-noise ratio (SNR) of measurements made with the final device, reducing its detection efficiency. In order to maximize this SNR it is necessary to match any cavity loss by using reflectors with similar transmittance [12]. Our cavities were found to exhibit relatively low throughput, with calculations indicating single-pass grating losses of 1%–2%, one order of magnitude higher than losses observed in comparable gratings at telecommunication wavelengths ($\sim$1550 nm). However, following thermal annealing to reduce the grating strength, a process well reported in the literature [15–17], we also observed a sevenfold decrease in the grating loss per unit length. The consequent increase in transmission and decrease in cavity loss will greatly improve the SNR of atom detection measurements.

This paper is organized as follows: Section II introduces the grating and cavity theory used to analyze the data and shows how the measurement SNR would compare with that for measurements made with an ideal device exhibiting no grating loss. The transmission measurement of a single grating from a cavity is detailed in Sec. III. In Sec. IV cavity characterization is explained and results given, showing excellent agreement in grating transmission between the two experiments which corroborates our results. Following this, details of the loss reduction caused by thermal annealing are given in Sec. V, and we conclude with a discussion of the underlying physics.

II. THEORY OF LOSSY FIBER BRAGG GRATING CAVITIES

The presence of a periodic perturbation (periodicity Λ) of the refractive index in the core of a single-mode optical fiber couples forward and backward guided modes [14]. Despite the relatively small index change of the perturbation, $\delta n_{\text{eff}} \sim 10^{-5}-10^{-3}$, the high number of periods and the phase matching at wavelengths close to the Bragg wavelength $\lambda_B = 2n_{\text{eff}}\Lambda$, where n_{eff} is the effective index of the fiber, can lead to extremely high reflectivity. The theoretical descrip-

tion of Bragg gratings is usually based on a coupled-mode equation approach, where the coupling constant κ between the forward and backward propagating fiber modes is calculated to lowest order in the weak index perturbation within the slowly varying amplitude approximation. By solving these coupled-mode equations, the amplitude reflection and transmission coefficients r and t, respectively, of a Bragg grating can be written as [18,19]

$$r = \frac{j\kappa \sinh(pZ)}{p\cosh(pZ) - j\sigma \sinh(pZ)} \tag{1}$$

and

$$t = \frac{p}{p\cosh(pZ) - j\sigma \sinh(pZ)}, \tag{2}$$

with

$$p = \sqrt{\kappa^2 - \sigma^2} \tag{3}$$

and

$$\kappa = \frac{\pi \delta n_{\text{eff}}}{\lambda_B}, \quad \sigma = \delta + j\alpha. \tag{4}$$

Here Z is the length of the grating and α is the amplitude loss per unit length which we assume constant throughout the grating. The detuning from the Bragg wavelength is defined as

$$\delta = 2n_{\text{eff}}\pi\left(\frac{1}{\lambda} - \frac{1}{\lambda_B}\right). \tag{5}$$

After expanding Eqs. (1) and (2) to first order in α/κ and defining the single-grating reflectivity $R=|r|^2$, transmission $T=|t|^2$, and loss $L=1-R-T$, we can express κ and α in terms of measurable quantities as

$$\tanh^2(\kappa Z) = \frac{R'}{1-L'} \tag{6}$$

and

$$\frac{\alpha}{\kappa} = \frac{1}{2}L'\sqrt{\frac{1-L'}{R'}}. \tag{7}$$

Here, R' is the maximum reflectivity which occurs at zero detuning $\delta=0$ ($\lambda=\lambda_B$) and L' is the grating loss at this wavelength.

Next we discuss the optical properties of a fiber Fabry-Perot cavity formed between two similar Bragg gratings. The cavity finesse is defined as the ratio of the separation between adjacent maxima to the full width at half the maximum of the resonance and can be written as [20]

$$F = \frac{\pi\sqrt{R}}{1-R}, \tag{8}$$

which for small $T+L$ can be expanded to give [21]

$$F = \frac{\pi}{T+L} - \frac{\pi}{2}. \tag{9}$$

The cavity throughput τ—i.e., the cavity transmission on resonance—can be written as

$$\tau = \frac{1}{(1+L/T)^2}, \tag{10}$$

where R, T, and L are the parameters for a single grating. For characterization purposes we make measurements on closed cavities (no gap), and as such we can attribute the single pass loss of the cavity as being due to the grating loss L only, neglecting the intrinsic fiber loss, since this is less than 10^{-4} over a single transit of the cavity. However, when considering a gap cavity, the loss L must encompass both grating loss and the loss due to the gap, L_{gap}. A measure of how the grating loss will affect the final device can be acquired by comparing the signal to noise $\mathcal{R}_{\text{SN}}$ of a measurement made with the cavity in question with the signal to noise, $\mathcal{R}_{\text{SN}_{\text{ideal}}}$, of a measurement made using an "ideal" cavity—one for which there is no grating loss and for which $T=L_{\text{gap}}$, maximizing $\mathcal{R}_{\text{SN}_{\text{ideal}}}$. Using the theory developed in the paper by Horak *et al.* [12] we consider a homodyne detection scheme and low atomic saturation for which we obtain a ratio

$$\epsilon(T,L) = \frac{\mathcal{R}_{\text{SN}}}{\mathcal{R}_{\text{SN}_{\text{ideal}}}} = 4\frac{TL_{\text{gap}}}{(T+L_{\text{gap}}+L)^2}. \tag{11}$$

This figure of merit, ϵ, is calculated for all cavities; the inverse $1/\epsilon$ gives the number of atoms needed in order to obtain the same signal-to-noise ratio as that obtained for the measurement of a single atom in the ideal case. It is also worth noting that, within this regime of low atomic saturation, although the signal-to-noise ratio increases with the square root of the input intensity, the number of spontaneously scattered photons increases proportionally with pump intensity. So increasing the pump power in order to gain a higher output signal will heat the atom more and be detrimental if we were to consider more sophisticated applications dependent on atomic coherences.

For clarity, we show a schematic of a fiber Bragg cavity transmission spectrum in Fig. 1(a). The envelope of the spectrum is given by the grating transmission $|t|^2$, Eq. (2). Within the grating band gap (of the order of 0.1 nm wavelength width), we observe much narrower cavity resonances with peaks given by the throughput τ. Experimentally, the throughput was obtained as the ratio of the resonant transmission to the transmitted power outside of the band gap. The finesse was calculated via $F=\text{FSR}/\text{FWHM}$, with FWHM being the full width at half of the maximum transmitted intensity ($\tau/2$) of the resonance peaks and FSR the free spectral range of the cavity, as illustrated in Fig. 1(b).

III. GRATING TRANSMISSION MEASUREMENTS

We fabricated four sets of cavities (which we denote by 1, 2, 3, and 4) with different writing parameters, each set consisting of three cavities (labeled a, b, and c). The cavities were manufactured by writing pairs of gratings in hydrogen-

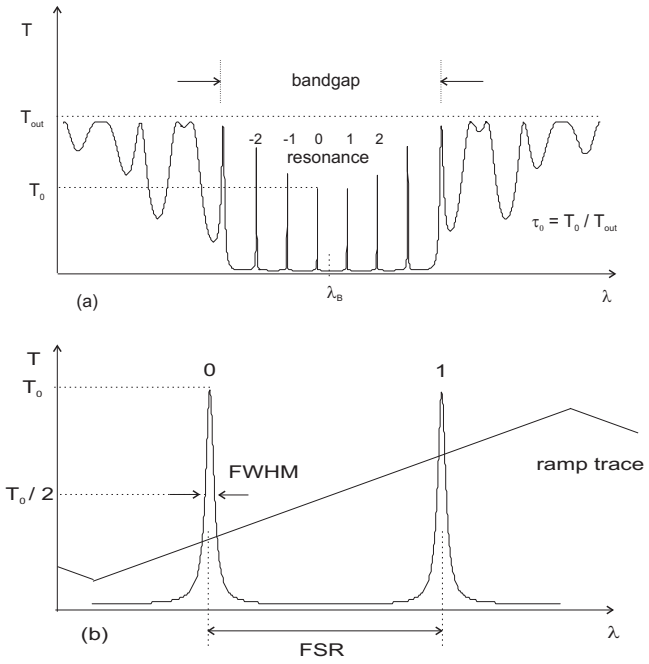

FIG. 1. (a) Illustration of the transmission spectrum of a fiber cavity with relevant throughput measurements and (b) pair of resonances used for finesse and throughput measurements (the finesse and peak transmission values for resonance 0 would be taken from the average of measurements made on the resonant pairs −1, 0 and 0, 1, for example). The ramp trace indicates the extent over which the wavelength is scanned.

ated single-mode boron/germanium codoped fiber (Fibercore PS750). Each cavity measured approximately 5 cm in length. Grating lengths varied from 2 to 5 mm and writing fluences from 150 to 800 J cm^{-2}; see Table I for details. The wavelength of the writing laser was 244 nm in all cases. To remove the hydrogen and thermally stabilize the gratings they were initially annealed at 100 °C for 19 h.

In a first experiment we measured the transmission spectrum of individual gratings. To this end, we stretched the other cavity grating in order to shift its Bragg wavelength away from that of the grating under investigation. From the measured spectra we then calculated the coupling strength κ. Moreover, comparing the results of the two gratings forming a cavity allowed us to identify any grating mismatch in strength and Bragg wavelength. Note that these effects are usually coupled: increasing the index modulation δn_{eff} increases the strength of the grating (κ is increased), but also increases the Bragg wavelength, as this is dependent on the average effective refractive index [14]. By stepping the laser wavelength discretely across the band gap, a measurement of the grating transmission was made using an optical spectrum analyzer set at its highest resolution (0.01 nm). A wavemeter was used for accurate absolute wavelength measurement and normalization purposes.

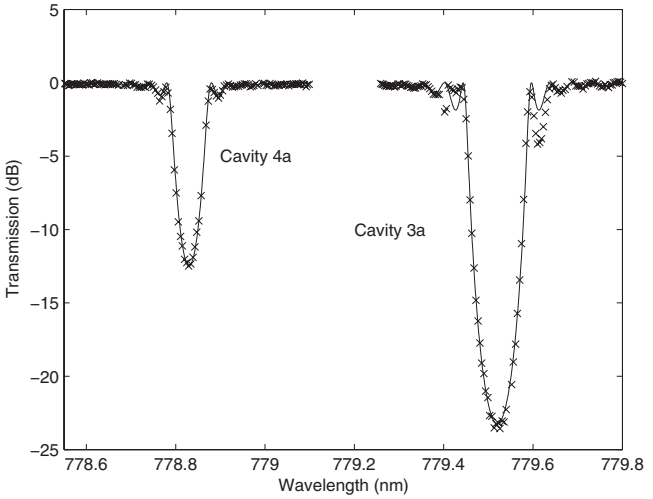

FIG. 2. Transmission spectra of a single grating from cavity 3a and cavity 4a. Solid lines are theoretical fits.

Figure 2 shows examples of the transmission spectra of individual gratings from cavities 3a and 4a, together with fits to the data using $|t|^2$ from Eq. (2) using the method of least squares. Since α is too small to have a visible effect on a

TABLE I. Grating parameters [length Z and writing fluence (WF)] as well as coupling and loss coefficients measured by two methods. Measurements [29] are an average of each pair. Note that the relatively large uncertainty in the cavity 1a measurement is due to a slight grating mismatch.

			Cavity measurement		Single-grating measurement
Cavity No.	Z (mm)	WF (J cm^{-2})	κ (m^{-1})	α (m^{-1})	κ (m^{-1})
1a	2	800	1217±15	3.6±0.6	1200±23
1b	2	800	1178±15	3.5±0.8	
1c	2	800	1217±15	3.6±0.6	
2a	5	150	415±4	3.4±0.3	407±5
2b	5	150	451±5	3.5±0.4	
3a	4	400	847±24	4.3±0.6	836±6
3b	4	400	912±25	5.1±0.7	
3c	4	400	894±25	4.9±0.7	
4a	5	185	418±6	3.5±0.2	410±14
4b	5	185	498±5	4.2±0.2	
4c	5	185	466±4	4.0±0.1	

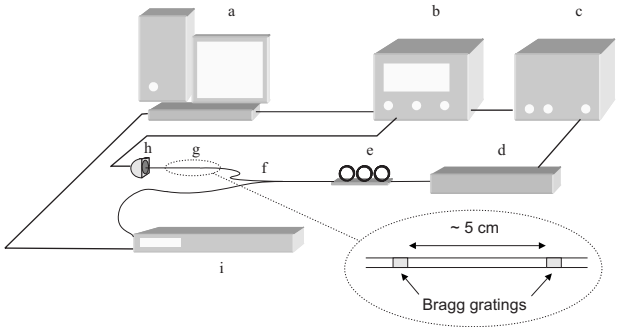

FIG. 3. Schematic of fiber cavity characterization setup: (a) PC, (b) oscilloscope, (c) function generator, (d) ECDL, free space optics, and fiber launch, (e) polarization control, (f) 50-50 coupler (port 4 terminated in index-matched fluid, not shown), (g) fiber cavity position, (h) photodiode, and (i) wavemeter.

single-path measurement, this was set to zero in order to obtain values for κ. We note that the fits accurately model the band gap and the minimum transmission, as well as some of the sidelobes of the spectra. The values for the coupling coefficient arising from the fit are $\kappa=836\ \mathrm{m}^{-1}$ and $\kappa=410\ \mathrm{m}^{-1}$ for cavity gratings 3a and 4a, respectively. Table I gives the values of κ for the first cavity in each set and comparative values from the cavity characterization measurements (see Sec. IV). The relatively large errors in the κ values for sets 1 and 4 are due to a slight grating mismatch in each cavity.

IV. CAVITY CHARACTERIZATION EXPERIMENT

As mentioned in the previous section, it is not possible to obtain a figure for the grating loss using the transmission data alone. In a second experiment, we have therefore characterized the cavity transmission, which is much more sensitive to losses due to the cavity enhancement. The measured cavity finesse and throughput can then be translated into information about the grating transmission and loss, as outlined in Sec. II. Agreement between the calculated values for the grating transmissions with the values obtained from the single-grating measurements gives weight to the calculated loss values.

The experimental setup used to characterize the cavities is shown in Fig. 3, and a diagram of the relevant features from a cavity transmission experiment is shown in Fig. 1. The experiment was performed using a tunable external cavity diode laser (ECDL), the intensity of the light transmitted through the cavity was measured by a photodiode, and the signal was displayed on a digital oscilloscope. Initially the band gaps of the cavities were identified by using the amplified spontaneous emission from the laser, in conjunction with an optical spectrum analyzer. Next, the wavelength of the ECDL was coarsely tuned to the grating band gap by manual adjustment of the ECDL grating, and finally the wavelength was scanned by applying a ramp voltage, or triangular wave, across the laser piezo. This ramp voltage was adjusted so that the ramp covered two free spectral ranges (FSR's) of the cavity; see Fig. 1(b). Normalization readings and absolute

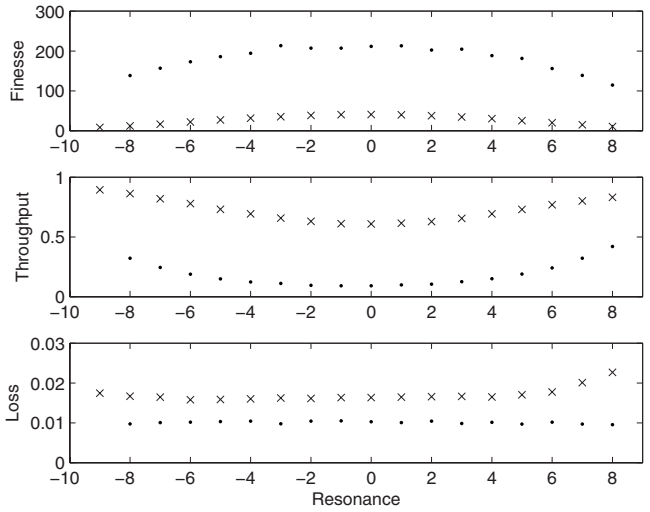

FIG. 4. Measured cavity finesse F, throughput τ, and calculated loss L for cavities 3a (dots) and 4a (crosses).

wavelength measurements were taken with a wavemeter. A LabView program read the oscilloscope and fitted pairs of Lorentzians to each of the resonant peaks on the traces. Where the FWHM values, or the amplitude values, of the data resonances differed from the fit by a set percentage, typically 5%, the measurements were rejected. The program was written to register ten values for the finesse and amplitude of the peaks for each pair of resonances in order to take an average and additionally record the power input to the wavemeter to normalize the throughput values.

Figure 4 shows the measured cavity finesse and throughput for cavities 3a and 4a over a range of cavity resonances close to the center of the grating band gaps. For wavelength-matched gratings, the highest cavity finesse occurs when $\delta \approx 0$—i.e., for the cavity resonance closest to the wavelength of maximum reflectance of the gratings. Any asymmetry in the cavity transmission peaks in this wavelength range points to a mismatch of the two cavity gratings. Using the measured values for finesse F and throughput τ we then calculate the single-grating transmission T and loss L by inverting Eqs. (9) and (10). The resulting loss values are shown in Fig. 4. We observe that the losses are nearly flat over the center of the grating band gap and are approximately 1.0% [29] and 1.6%, respectively, for the two cavities.

Table II summarizes the maximum finesse measurements for all our cavities, in addition to the corresponding cavity throughputs, calculated losses, and grating transmissions. The errors in the finesse and the throughput measurements are taken to be the standard deviations from their respective mean values, with the relative uncertainties of the calculated loss and transmission obtained by

$$\frac{\Delta L}{L} = \left\{ \frac{\Delta\tau^2}{4\tau(1-\sqrt{\tau})^2} + \frac{\Delta F^2}{(F+\pi/2)^2} \right\}^{1/2} \tag{12}$$

and

$$\frac{\Delta T}{T} = \left\{ \frac{\Delta\tau^2}{4\tau^2} + \frac{\Delta F^2}{(F+\pi/2)^2} \right\}^{1/2}. \tag{13}$$

TABLE II. Measurements [29] and calculations from all cavities.

	Measured		Calculated		
Cavity No.	Finesse	Throughput (%)	Grating loss ($\times 10^{-3}$)	Grating transmission (dB)	ϵ
1a	85.7±4.3	70±4	5.9±1.0	−15.2±0.3	0.64
1b[a]	75.1±3.5	73±5	5.9±1.3	−14.5±0.3	0.61
1c	85.9±4.3	70±5	5.9±1.0	−15.2±0.3	0.64
2a	39.5±1.0	62±3	16.0±1.5	−12.2±0.1	0.38
2b	52.9±1.6	54±4	15.3±1.7	−13.7±0.2	0.43
3a	211.5±34.8	9.3±1.8	10.2±1.7	−23.5±0.9	0.30
3b	225.1±37.6	3.7±0.8	11.2±1.9	−25.7±1.0	0.19
3c	223.4±38.3	4.9±0.9	10.9±1.9	−25.1±0.9	0.22
4a	40.7±2.1	62±2	16.0±1.3	−12.3±0.2	0.38
4b	70.7±2.5	38±2	16.8±0.9	−15.7±0.2	0.42
4c	57.0±1.5	47±2	17.0±0.9	−14.4±0.2	0.42

[a]Grating mismatch.

We use Eqs. (6) and (7) to calculate the grating coupling strength κ and loss coefficients α, respectively. The results are shown in Table I. We find excellent agreement between the fitted values of κ from the transmission measurements (Sec. III) and the calculated values of κ from the cavity measurements, with the difference being well within the measurement uncertainties. This gives confidence in the grating loss values calculated from the cavity measurements.

The grating loss is of the order of 1%–2% for all our cavities, with the grating loss coefficients calculated to be in the range of 3–5 m^{-1}. While there is a strong correlation of the grating strength κ with the writing fluence as expected (see Table I), there appears to be no simple relation of the loss coefficient α to the fabrication parameters. In this case of essentially constant loss coefficients, the lowest losses per pass are achieved for the gratings with the largest values of κ. This can be seen from Table II and can also be derived theoretically from Eqs. (1) and (2). The physical reason for this dependence is that for stronger coupling coefficients light is reflected within a shorter distance of propagation in the grating and therefore the loss per reflection is smaller.

If we consider the values for ϵ for each cavity given in the last column of Table II, it appears that the grating loss will prohibit single-atom detection for a gap cavity device in all cases; however, this is not the case. The SNR for a homodyne detection measurement is proportional to the square root of the detection time, so effectively a value of $\epsilon=0.5$ means that the detection time would need to be increased fourfold in order to obtain $\mathcal{R}_{\mathrm{SN}_{\mathrm{ideal}}}$, for a constant input photon rate. This time increase, however, will entail a fourfold increase in the number of spontaneously scattered photons for the same input rate. Alternatively, all the cavities would be suitable for the detection of small numbers of atoms without increasing the detection time. It is also worth noting that the cooperativity parameter, which describes the ratio of coherent atom-field coupling to dissipative atomic and cavity damping, is of the order of unity for the cavities discussed in this paper, once the gap has been introduced. Therefore our final device will be only slightly below the strong-coupling regime of cavity quantum electrodynamics required for quantum nondemolition measurements.

Finally, for comparison we note that measurements on a similar cavity written in standard telecommunication fiber at 1550 nm resulted in a grating transmission of $T=-19.1$ dB and a single pass loss of $L=0.0019$ or, equivalently, $\kappa=578$ m^{-1} with a loss per unit length of $\alpha=0.6$ m^{-1}. We thus conclude that our 780-nm gratings exhibit losses one order of magnitude larger than comparable gratings at 1550 nm.

V. ANNEALING EXPERIMENT

For applications in atom chips and, more generally, in quantum information processing, these losses are prohibitively high, and techniques to reduce these losses have to be found. The throughput for the highest finesse cavities, set 3, was low due to the grating loss. This grating loss also gives a value for ϵ that indicates that we would need four or five atoms in the cavity to obtain a similar SNR as that for single-atom detection in the ideal case. A reduction in grating strength will increase this transmission and hence improve the throughput and signal-to-noise ratio for measurements made using these cavities. Partial annealing of Bragg gratings by heating is well known [15–17], and we therefore performed an experiment in order to find the required combination of temperature and time needed to reduce the strength of the gratings by a specified amount. As a result of this, the grating strength was reduced as expected; however, there was also a marked reduction in the grating loss.

For this experiment, the cavity was placed on a hot plate at a certain temperature for a set amount of time, then removed, and characterized as before. The fiber cavity was then returned to the hot plate for another prescribed time period and the procedure was repeated. Figure 5 shows the results for the annealing of cavity 3a. Initially, the hot plate was set to a temperature of 200 °C. After 1 h, the grating transmission was increased from −23.5 dB to −19.2 dB and

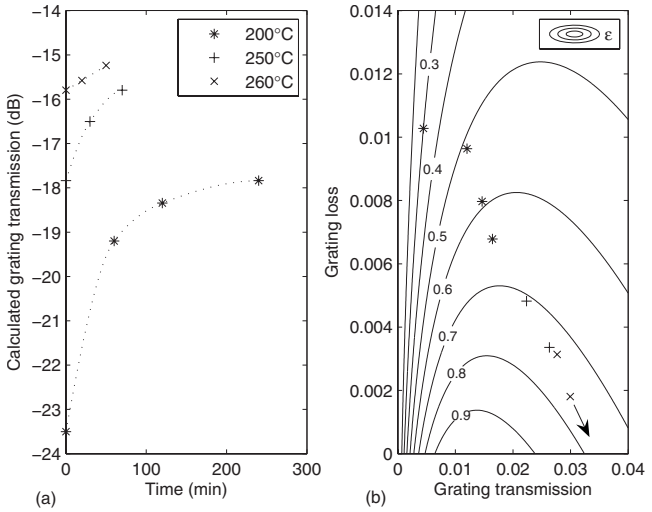

FIG. 5. Results of thermal annealing of cavity 3a. (a) Grating transmission T depending on annealing temperature and duration (the dotted lines provide a guide only). (b) Calculated grating loss L and transmission T against ϵ (contours). Arrow indicates annealing trend. The data point legend applies to both graphs.

after another 3 h to −17.8 dB. At this point, the annealing became slow and the temperature was increased to 250 °C to accelerate the process. The transmission of the grating was thus increased to −15.8 dB and finally to −15.2 dB at temperatures of 260 °C.

As expected the maximum cavity finesse was reduced due to the increased grating transmission, from $F \approx 200$ to $F \approx 100$ over the extent of the experiment. However, more importantly, we observed a reduction of grating loss from 1.0% per pass to 0.2%, as seen in Fig. 5(b). For our targeted application of fiber cavities for single-atom detection on an atom chip, this significant improvement in grating performance means that losses are now smaller than the intrinsic diffraction loss in the cavity gap required to accommodate the atom. Therefore the device sensitivity will no longer be limited by the quality of the Bragg gratings. Figure 5(b) shows the trend in ϵ as the experiment progressed, with ϵ increasing from 0.30 to 0.76. Using again Eqs. (6) and (7) we find that the loss per unit length was reduced from $\alpha = 4.3\ \mathrm{m}^{-1}$ to $\alpha = 0.6\ \mathrm{m}^{-1}$ after the full annealing. We note that the magnitude of the final value is now equivalent to the value calculated for the 1550-nm cavity. At the same time, annealing only reduced the coupling strength of the grating from $\kappa = 848\ \mathrm{m}^{-1}$ to $610\ \mathrm{m}^{-1}$—i.e., by about 28%.

VI. DISCUSSION AND SUMMARY

Let us now discuss the origin of these losses in UV-written gratings. First we note that the losses cannot be assumed to arise solely from scattering. Scattering losses for boron-germanium-codoped fiber in strong gratings ($R > 0.97$) at 1535 nm wavelength have been measured by Janos *et al.* [22] to be $(5-30) \times 10^{-5}$ dB cm^{-1}. Considering the usual wavelength scaling of Rayleigh scattering as $1/\lambda^4$, this equates to $\alpha = 0.02-0.1\ \mathrm{m}^{-1}$ at 780 nm and is therefore about two orders of magnitude too small to account for our observed losses.

Absorption losses, on the other hand, are known to increase strongly for shorter wavelengths in germano-silicate fibers because of absorption bands in the UV at about 240 nm. Losses comparable to $\alpha = 4\ \mathrm{m}^{-1}$ measured here have been reported previously [23,24]. Askins and Putnam [23] have shown that these losses can be reduced by photobleaching while the corresponding reduction in grating reflectivity is relatively minor, similar to our results reported here for thermal annealing. Anoikin *et al.* [24] have also reported thermal annealing to reduce grating losses at temperatures larger than 200 °C. These losses have been attributed to the creation of paramagnetic Ge(1) centers in the fiber. In contrast to these previous studies where gratings were fabricated using pulsed excimer lasers, our gratings are written by a cw UV source. Because of the much lower peak powers in this case, one might have expected to induce fewer color centers in the germano-silicate matrix; however, this appears not to be the case. Moreover, our results show that the absorption rate is hardly affected by increasing the writing fluence from 150 to 800 J cm^{-2}. This suggests that the majority of color centers are created at very low UV intensities and that this photodarkening effect quickly saturates at higher UV exposures. Heating of the gratings to 200–260 °C for times of the order of 1 h proved to be an efficient method to reduce these losses. At the same time, this thermal processing only weakly affects the structural changes of the glass matrix responsible for the refractive index grating [25], as evidenced by the relatively modest reduction in grating strength in our annealing experiment.

In summary, we have investigated fiber Bragg cavities side-written by cw UV light in hydrogenated boron-germanium-codoped single-mode fiber. In particular, we have been interested in the suitability of such resonators for atom chip applications using rubidium atoms—that is, at wavelengths of 780 nm. We found that after the UV writing, the gratings exhibited large losses of 1%–2% per pass and corresponding loss coefficients of the order of 4 m^{-1}. Thermal annealing of the gratings reduced the loss coefficient to 0.6 m^{-1}. The concurrent increase in the figure of merit, ϵ, to 0.76, indicates that we can construct a final device for which the SNR of atom detection measurements will approach that of an ideal device; i.e., it will be sensitive enough for single-atom detection. With further optimization of the fabrication process we expect to achieve much higher closed-cavity finesses. This will be of interest for atom chip experiments and for other sensor applications where particles interact with the evanescent field (similar to microsphere or microdisk [26–28] proposals) of the fiber mode rather than with the field inside a gap. While such a geometry reduces the particle-light coupling strength due to the lower field intensity outside the fiber core, it will significantly simplify mounting and aligning such a device.

We therefore conclude that Bragg cavities are a viable technology for quantum information processing when working at wavelengths close to 780 nm, provided that they are fabricated by a two-step process, where initial UV writing of extremely strong gratings is followed by thermal processing to reduce grating losses and to adjust the transmission to the required value.

[1] R. Folman, P. Krüger, J. Schmiedmayer, J. Denschlag, and C. Henkel, Adv. At., Mol., Opt. Phys. **48**, 263 (2002).
[2] J. Schmiedmayer, R. Folman, and T. Calarco, J. Mod. Opt. **49**, 1375 (2002).
[3] J. Reichel, Appl. Phys. B: Lasers Opt. **74**, 469 (2002).
[4] K. Brugger, T. Calarco, D. Cassettari, R. Folman, A. Haase, B. Hessmo, P. Krüger, T. Maier, and J. Schmiedmayer, J. Mod. Opt. **47**, 2789 (2000).
[5] C. D. J. Sinclair, E. A. Curtis, I. Llorente Garcia, J. A. Retter, B. V. Hall, S. Eriksson, B. E. Sauer, and E. A. Hinds, Phys. Rev. A **72**, 031603(R) (2005).
[6] A. Haase, B. Hessmo, and J. Schmiedmayer, Opt. Lett. **31**, 268 (2006).
[7] I. Teper, Y.-J. Lin, and Vladan Vuletić, Phys. Rev. Lett. **97**, 023002 (2006).
[8] S. Eriksson, M. Trupke, H. F. Powell, D. Sahagun, C. D. J. Sinclair, E. A. Curtis, B. E. Sauer, E. A. Hinds, Z. Moktadir, C. O. Gollasch, and M. Kraft, Eur. Phys. J. D **35**, 135 (2005).
[9] X. Liu, K.-H. Brenner, M. Wilzbach, M. Schwarz, T. Fernholz, and J. Schmiedmayer, Appl. Opt. **44**, 6857 (2005).
[10] P. A. Quinto-Su, M. Tscherneck, M. Holmes, and N. P. Bigelow, Opt. Express **12**, 5098 (2004).
[11] R. Long, T. Steinmetz, P. Hommelhoff, W. Hänsel, T. W. Hänsch, and J. Reichel, Philos. Trans. R. Soc. London, Ser. A **361**, 1375 (2003).
[12] P. Horak, B. G. Klappauf, A. Haase, R. Folman, J. Schmiedmayer, P. Domokos, and E. A. Hinds, Phys. Rev. A **67**, 043806 (2003).
[13] K. O. Hill and G. Meltz, J. Lightwave Technol. **15**, 1263 (1997).
[14] R. Kashyap, *Fiber Bragg Gratings* (Academic Press, San Diego, 1999).
[15] K. E. Chisholm, K. Sugden, and I. Bennion, J. Phys. D **31**, 61 (1998).
[16] H. Patrick, S. L. Gibert, A. Lidgard, and M. D. Gallagher, J. Appl. Phys. **78**, 2940 (1995).
[17] S. R. Baker, H. N. Rouke, V. Baker, and D. Goodchild, J. Lightwave Technol. **15**, 1470 (1997).
[18] T. Erdogan, J. Lightwave Technol. **15**, 1277 (1997).
[19] V. Finazzi and M. N. Zervas, Appl. Opt. **41**, 2240 (2002).
[20] E. Hecht, *Optics*, 3rd ed. (Addison-Wesley, New York, 1998).
[21] J. Stone and D. Marcuse, J. Lightwave Technol. **4**, 382 (1986).
[22] M. Janos, J. Canning, and M. G. Sceats, Opt. Lett. **21**, 1827 (1996).
[23] C. G. Askins and M. A. Putnam, J. Lightwave Technol. **15**, 1363 (1997).
[24] E. V. Anoikin, V. M. Mashinsky, V. B. Neustruev, and Y. S. Sidorin, J. Non-Cryst. Solids **179**, 243 (1994).
[25] B. Poumellec and F. Kherbouche, J. Phys. III **6**, 1595 (1996).
[26] M. Rosenblit, P. Horak, S. Helsby, and R. Folman, Phys. Rev. A **70**, 053808 (2004).
[27] M. Rosenblit, Y. Japha, P. Horak, and R. Folman, Phys. Rev. A **73**, 063805 (2006).
[28] P. Barclay, K. Srinivasan, O. Painter, B. Lev, and H. Mabuchi, Appl. Phys. Lett. **89**, 0131108 (2006).
[29] The quoted values for finesse and throughput take into account the equipment response and laser linewidth.